Journal of Clinical and Translational Hepatology **2022**
DOI: 10.14218/JCTH.2022.00060

Original Article

USP10 Alleviates Palmitic Acid-induced Steatosis through Autophagy in HepG2 Cells

Sheng-Liang Xin[1], Xiao-Li Pan[2], Xiao-Yuan Xu[1] and Yan-Yan Yu[1*]

[1]*Department of Infectious Diseases, Peking University First Hospital, Beijing, China;* [2]*Division of Gastroenterology, Union Hospital, Tongji Medical College, Huazhong University of Science and Technology, Wuhan, Hubei, China*

Received: 6 February 2022 | **Revised:** 3 March 2022 | **Accepted:** 21 March 2022 | **Published:** 31 March 2022

Abstract

Background and Aims: Nonalcoholic fatty liver disease (NAFLD) is a common chronic liver disease caused by overnutrition. Impaired autophagy is closely related to NAFLD progression. Recently, ubiquitin-specific peptidase-10 (USP10) was reported to ameliorate hepatic steatosis, but the underlying mechanism is still unclear. In view of the potential effects of USP10 on autophagy, we investigated whether USP10 alleviated steatosis through autophagy. ***Methods:*** HepG2 cells were treated with palmitic acid (PA) to model NAFLD *in vitro*. Lentivirus was used to regulate USP10 level in cells. Autophagic regulators were used to autophagic progression in cells. Western blotting, real-time fluorescence quantitative polymerase chain reaction, lipid drop staining and immunofluorescent staining were performed to determine the effect of USP10 on lipid autophagy. Student's *t*-test and Tukey's post hoc test were used to compare the means among groups. ***Results:*** PA induced cellular steatosis with dependance on autophagy. USP10 overexpression alleviated PA-induced steatosis, restored autophagic activity, promoted autophagic flux, including synthesis and degradation of autophagosomes, and lipid-targeted autophagy. In the presence of autophagy inhibitors, the protective effectiveness of USP10 on steatosis decreased. Furthermore, the specific inhibitor to C-jun N-terminal protein kinase-1 (JNK1), DB07268, abolished USP10-induced autophagy. However, during early stage inhibition of JNK1, compensatory expression of tuberous sclerosis complex-2 (TSC2) maintained autophagy. The degree of TSC2-to-JNK1 compensation was positively associated with USP10 level. Functionally, JNK1 and TSC2 were involved in the lipid-lowering effect of USP10. ***Conclusions:*** USP10 alleviated hepatocellular steatosis in autophagy-dependent manner. JNK1/TSC2 signaling pathways were required for USP10-induced autophagy.

Citation of this article: Xin SL, Pan XL, Xu XY, Yu YY. USP10 Alleviates Palmitic Acid-induced Steatosis through Autophagy in HepG2 Cells. J Clin Transl Hepatol 2022. doi: 10.14218/JCTH.2022.00060.

Keywords: Autophagy; Nonalcoholic fatty liver disease; Steatosis; Ubiquitin-specific peptidase-10; C-jun N-terminal protein kinase-1; Tuberous sclerosis complex-2.

Abbreviations: 3-MA, 3-Methyladenine; AMPK, AMP-activated protein kinase; ATGs, autophagy target genes; Baf A1, bafilomycin A1; CCK-8, cell counting kit-8; CQ, chloroquine diphosphate salt; DAPI, 4′,6-diamidino-2-phenylindole; DMEM, Dulbecco's modified eagle medium; EBSS, Earle's balanced salt solution; JNK, C-jun N-terminal protein kinase; LAMP, lysosomal associated membrane protein; LC, microtubule-associated protein light chain; LDs, lipid drops; MOI, multiplicity of infection; mTOR, mammalian target of rapamycin; NAFLD, non-alcoholic fatty liver disease; NASH, non-alcoholic steatohepatitis; NS, no significant difference; PA, palmitic acid; PBS, phosphate buffer saline; q-PCR, real-time fluorescence quantitative polymerase chain reaction; S6K, ribosomal protein S6 kinase; SD, standard deviation; TSC, tuberous sclerosis complex; ULK, unc-51 like autophagy activating kinase; USP, ubiquitin-specific peptidase; Veh, vehicle; VPS34, Phosphatidylinositol 3-kinase.

[*]**Correspondence to:** Yan-Yan Yu, Department of Infectious Diseases, Peking University First Hospital, Xishiku Street NO.8, Beijing 100034, China. ORCID: https://orcid.org/0000-0002-7557-1305. Tel: +86-10-66551066, Fax: +86-10-83572022, E-mail: yyy@bjmu.edu.cn

Introduction

Nonalcoholic fatty liver disease (NAFLD) is the most common chronic liver disease worldwide, including developing countries. NAFLD is a metabolic disease, with significant accumulation of lipid droplets (LDs) in hepatocytes that is usually associated with oxidative stress, inflammation, fibrogenesis, and insulin resistance. Progressive NAFLD can develop into nonalcoholic steatohepatitis (NASH) or hepatocellular carcinoma. NAFLD accompanied with obesity, type 2 diabetes mellitus, and cardiovascular events increases overall mortality.[1] NAFLD has become the most frequent indication for liver transplantation.[2] An international expert consensus recommended renaming NAFLD as metabolic dysfunction-associated fatty liver disease.[3] The pathogenesis of NAFLD is unclear and the treatment of NAFLD is limited.

Autophagy is a highly conserved intracellular activity that degrades cellular components, such as impaired organelles and redundant metabolites. The classic autophagy process starts with the synthesis of autophagosomes. Microtubule-associated protein light chain (LC)3B-1, the inactive form of LC3B, located in cytosol, is recruited to membranes of autophagosomes and convert to its active form, LC3B-2. Target substances are engulfed by autophagosomes, which then fuse with lysosomes to form autolysosomes, in which the engulfed substances are degraded.[4] Autophagy is regulated by a cluster of autophagy target genes (ATGs) and is induced by energic stress and messengers like AMP-activated protein kinase (AMPK).[5] Lack of ATG5[6] or ATG7[7] and autophagic inhibitors[6] increases the concentration of triglyceride in hepatocytes. Palmitate acid (PA) has been shown to suppress autophagy in hepatocytes in a time-dependent manner.[8] Some compounds that promote autophagy alleviate hepatic steatosis.[9,10] Therefore, autophagy plays a key role in NAFLD progression.

Ubiquitin-specific peptidase (USP)-10 is a deubiquitinating enzyme located in both the cytoplasm and nucleus,[11] and

its therapeutic effects on oxidative stress, infection, heat shock,[12,13] cardiac hypertrophy,[14] and hepatic ischemic/reperfusion injury[15] have been studied. The protective effects of USP10 in NAFLD, include inhibition of hepatic steatosis, insulin resistance, and inflammation via sirtuin-6.[16] USP10 is regulated by the long noncoding RNA Mirt2 and micro (mi)RNA-34a-5p to suppress hepatic steatosis.[17] USP10 interacts with Beclin1, a member of the autophagic complex, to stabilize p53 and inhibit cell proliferation,[18] and LC3B ubiquitination is reversed in H4 cells by USP10.[19] However, the direct role of USP10 in autophagy in NAFLD is unclear. Recently, positive feedback was found between USP10 and AMPK,[20] and we speculated that USP10 could directly regulate autophagy to alleviate hepatic steatosis. In this study, HepG2 cells were treated with PA to model NAFLD *in vitro*. HepG2 cells are suitable experimental NAFLD models because their biological and genetic characteristics.[21,22] PA is the most abundant unsaturated fatty acid in humans. USP10 expression was regulated by lentivirus infection. The results confirmed the underlying mechanism of the protective effects of USP10 on autophagic activity, autophagic flux, lipid-targeted autophagy in hepatic steatosis.

Methods

Reagents

PA solution was purchased from KunChuang (cat. no. 4; Xi'an, China). Hematoxylin (cat. no. 517-28-2), Oil Red O (cat. no. G1260), Bafilomycin A1 (cat. no. A8510), and Earle's balanced salt solution (EBSS) (cat. no. H2020) were purchased from Solarbio (Beijing, China). Chloroquine diphosphate salt (CQ) (cat. no. C6628) was purchased from Sigma-Aldrich (St. Louis, MO, USA). 3-Methyladenine (3-MA) (cat. no. HY-19312), rapamycin (cat. no. HY-10219), and DB07268 (cat. no. HY-15737) were purchased from MedChemExpress (Monmouth Junction, NJ, USA). Dulbecco's modified Eagle's medium (DMEM) (cat. no. 11965092), fetal bovine serum (cat. no. 12483020), and penicillin–streptomycin (cat. no. 15070063) were purchased from Gibco (Waltham, MA, USA). Phosphate buffered saline (PBS) (cat. no. G4202) was purchased from Servicebio (Wuhan, China).

Cell culture and treatment

HepG2 human hepatoma cells (GeneChem, Shanghai, China) were cultured in DMEM supplemented with 10% fetal bovine serum, 100 U/mL penicillin and 100 μg/mL streptomycin 37°C in humidified air containing 5% CO_2. PA and vehicle were diluted in culture medium to 125–500 μM for treatment. Before PA treatment, HepG2 cells were incubated with CQ (50 μM for 6 h), 3-MA (5 mM for 6 h), EBSS (2 h), bafilomycin A1 (100 nM for 5 h) and rapamycin (1 μM for 5 h). During PA treatment, HepG2 cells were co-incubated with DB07268 (1–216 μM).

Oil Red O staining

HepG2 cells were seeded in six-well plates at 2.5×10^5 cells/mL and treated with PA (125–500 μM) and vehicle for 24 h when they reached 50% confluence. Before PA or vehicle treatment, cells were pretreated with 3-MA or shATG5. After treatment, the cultures were washed three times with PBS, and the cells were fixed with 10% formalin for 20 m, washed three times with PBS, and stained with Oil Red O solution for 30 m. Cells were then washed three times with PBS and photographed. To quantify the extent of steatosis, LDs in cells were dissolved in isopropanol and absorbance of eluates at 520 nm was read with a microplate reader.

Triglyceride assay

The concentration of triglycerides in HepG2 cells was determined with a triglyceride quantification kit (cat. no. E1013; Applygen, Beijing, China).

Cell viability assay

The cytotoxicity of PA, vehicle, and DB07268 was measured by cell counting kit-8 (CCK-8) assays. Briefly, 1×10^4 cells/well were seeded in 96-well plates overnight and treated by PA (125–500 μM), vehicle, or co-incubated with DB07268 (1–216 μM) for 24 h. CCK-8 (cat. no. C0037; Beyotime, Beijing, China) was added to each well and the plates were incubated for an additional 1 h. The absorbance of the cultures was measured at 450 nm with a microplate reader.

Quantitative real-time fluorescence polymerase chain reaction (qPCR)

HepG2 cells were seeded in 12-well plates at 5×10^5 cells/mL and treated with PA (312.5 μM), vehicle, or co-incubated with DB07268 (9–45 μM) when they reached 70% confluence. Total RNA was extracted using RNAiso Plus (cat. no. 9108; Takara, Tokyo, Japan) PrimeScript RT reagent kit (Perfect Real Time, cat. no. RR037; Takara) was used to reverse transcribe RNA to cDNA. qPCR was performed on an Applied Biosystems 7500 Real-Time PCR System (Hercules, CA, USA) using TB Green Premix Ex*Taq* (Tli RNaseH Plus, cat. no. RR420; Takara). The qPCR total reaction volume was 20 μL, including TB Green Premix Ex*Taq* 10 μL, forward primer 10 μM 0.4 mL, reverse primer 10 μM 0.4 μL, ROX Reference Dye II (50×) 0.4 μL, DNA templates 50 ng/μL and sterile water 6.8 μL. qPCR cycling included three stages: 1, 95°C for 30 s; 2, 40 cycles of 95°C for 5 s, 55°C for 30 s and 72°C for 30 s; 3, 95°C for 15 s, 60°C for 60 s and 95°C for 15 s. Primers were provided by Tianyi Huiyuan Biotech Co. Ltd. (Beijing, China). The sequences are shown in Supplementary Table 1.

Western blotting

HepG2 cells were seeded in 12-well plates at 5×10^5 cells/mL and treated with PA (312.5 μM), vehicle, or co-incubated with DB07268 (9–45 μM) when they reached 70% confluence. Total protein was extracted using 1× sodium dodecyl sulfate (SDS)-polyacrylamide denaturing protein loading buffer (cat. no. B1012; Applygen) supplemented with 1× phosphatase inhibitor mixture (cat. no. P1260; Applygen). As LC3B-2 is easily degraded when outside cells, western blotting was performed after extraction of total protein. Equal amounts of cellular proteins were resolved by 6–15% SDS-polyacrylamide gel electrophoresis and transferred to polyvinylidene fluoride membranes (cat. no. IPVH00010; Merck Millipore, Burlington, MA, USA). Membranes were blocked with 5% bovine serum albumen (cat. no. G5002; Servicebio, Wuhan, China) for 1 h or QuickBlock (cat. no. P0252; Beyotime) for 10 m and incubated overnight at 4°C with specific primary antibodies (1:1,000). Antibodies to glyceraldehyde-3-phosphate dehydrogenase (cat. no. GB11002) and α-tubulin (cat. no. GB11200) were provided

by Servicebio. Antibody to β-actin (cat. no. AF5003) was provided by Beyotime. Antibody to USP10 (cat. no. ab109219) was provided by Abcam (Cambridge, MA, USA). Antibodies to LC3B (cat. no. 2775), lysosomal-associated membrane protein (LAMP)1 (cat. no. 9091), ATG14 (cat. no. 5504), mammalian target of rapamycin (mTOR) (cat. no. 2972) and p-mTOR at Ser2448 (cat. no. 2971) were provided by Cell Signaling Technology (CST) (Danvers, MA, USA). Antibodies to ATG5 (cat. no. A0203), Beclin1 (cat. no. A11761), tuberous sclerosis complex (TSC)2 (cat. no. A19540), C-jun N-terminal protein kinase-1 (JNK1) (cat. no. A0288), phosphatidylinositol 3-kinase (VPS34) (cat. no. A12295), B-cell lymphoma 2 (Bcl2) (cat. no. A19693), p-Bcl2 at Ser70 (cat. no. AP0575), ribosomal protein S6 kinase (S6K) (cat. no. A4898), p-S6K at Thr389 (cat. no. AP1059) and p62 (cat. no. A7758) were provided by ABclonal (Woburn, MA, USA). After incubation, membranes were probed with secondary antibodies (cat. no. A0208; Beyotime) for 1 h at room temperature. Signals were read with a super enhanced chemiluminescence detection kit (cat. no. NE0102; NovovBio, Beijing, China). Specific protein bands were visualized with a Syngene imaging system and gray values were measured with Image J software.

Lentiviral infection and stable cell line establishment

Lentiviral vectors were synthesized by Shanghai Jikai Gene Chemical Technology Co., Ltd (Shanghai, China). For USP10 RNA interference, three pairs of short hairpins were designed and their target sequences (5′ to 3′) were shUSP10 4-1 ccCATGATAGACAGCTTTGTT, shUSP10 5-1, ccTATGTGGAAACTAAGTATT, and shUSP10 6-1 gcTGTGGATAAACTACCTGAT. They were cloned into the lentiviral vector GV344. Interfering RNAs for ATG5 (effective target sequence 5′ to 3′ ccTGAACAGAATCATCCTTAA) and TSC2 (effective target sequence 5′ to 3′ cgACGAGTCAAACAAGCCAAT) were also synthesized. They were cloned into the lentiviral vector GV248. A recombinant lentiviral vector expressing a scrambled shRNA was used as a negative control. Lentiviral vectors caring USP10 sequence were also synthesized. Lentivirus particles were used to infect HepG2 cells and establish stable cell lines. To select positive cells, 2 μg/mL puromycin or flow-cytometric sorting was applied. Infection efficiency was confirmed by western blotting and Q-PCR.

Fluorescence staining

HepG2 cells were seeded on in six-well plates at 2.5×10^5 cells/mL and treated with PA (312.5 μM) or vehicle for 24 h, or additional by EBSS, rapamycin, CQ, 3-MA, bafilomycin A1, or DB07260 when they reached 30% confluence. After treatment, HepG2 cells were harvested and washed three times with PBS. The cells were fixed with 4% paraformaldehyde for 20 m, washed with PBS, and stained with BODIPY 493/503 (cat. no. GC42959; GLPBIO, Montclair, CA, USA) 0.5 μg/mL at room temperature. Tyramide signal amplification (TSA) was used to detect immunofluorescence in cells. HepG2 cells were deparaffinized and rehydrated. After antigen retrieval, blocking of endogenous peroxidases, and blocking with serum, they were incubated primary antibodies: anti-LC3B 1:200 (cat. no. 3868; CST); anti-LAMP1 1:50 (cat. no. 9001; CST); anti-USP10 1:50 (cat. no. ab109219; Abcam); and anti-TSC2 1:50 (cat. no. A19540; ABclonal). They were then incubated with horseradish peroxidase-labeled secondary antibodies, Cy3-TSA, or fluorescein isothiocyanate conjugated-TSA, with microwave treatment, the second round of primary antibodies and secondary antibodies incubation, and spontaneous fluorescence quenching. After stained with Bodipy 493/503 or antibodies, the nuclei of HepG2 were stained with 4′,6-diamidino-2-phenylindole (DAPI) at room temperature for 10 m. The cells were washed three times with PBS, cover slipped using anti-fade mounting medium, and observed by fluorescence microscopy and photographed. Details of fluorescent staining are described in the Servicebio protocol.

Statistical analysis

The results were reported as means±SD and the sample size reported for each procedure corresponds to number of results obtained from at least replicates. Between-group comparisons were performed with independent sample *t*-tests. Comparisons among three or more groups were performed with one-way analysis of variance followed by Tukey's *post hoc* test. Differences were considered statistically significant when p was <0.05. GraphPad Prism 8 software was used for the statistical analysis.

Results

Establishing an NAFLD cell model by PA treatment

HepG2 cells were treated with PA (125–500 μM) for 24 h, and compared with vehicle treatment, the number of LDs (Oil red O staining) and the triglyceride concentration (triglyceride assay) in HepG2 cells were increased by PA (Supplementary Fig. 1A, B). PA induced cellular steatosis in HepG2 cells. LDs induce lipotoxic effects in cells, with release of reactive oxygen species (ROS), which promotes NAFLD progression as a precursor.[23,24] A previous study found that ROS reaction was inducible when hepatocellular viability decreased to 50% under PA stimulation.[25] In this study, cellular viability of HepG2 cells decreased in PA groups with dose-independence (Supplementary Fig. 1C). Compared with the blank control group, cell viability as reduced by 250–375 μM PA (Supplementary Fig. 1C). We thus used the mean of 312.5 μM as the PA concentration for the modeling NAFLD in subsequent experiments.

PA affected USP10 expression and autophagic activity of HepG2 cells in a time-dependent manner

Cells were harvested at 6, 12, and 24 h during PA stimulation. Representative molecules were detected to reflect different stages of autophagy, including induction of autophagy. They were Beclin1 and ATG14), synthesis of autophagosomes [ATG5, ATG7, and unc-51 like autophagy activating kinase (ULK1),[4] autophagosome marker (LC3B),[4] substrate of autophagy (p62),[4] and degradation of autophagosomes (LAMP1). *USP10* gene expression decreased successively during PA stimulation (Fig. 1A). *LC3B, p62, LAMP1, ULK1, ATG7*, and *ATG14* gene expression increased at 6–12 h and then decreased at 24 h (Fig. 1A). USP10 protein expression decreased significantly at 24 h. ATG5, Beclin1 and LC3B-2 protein expression increased at 6 h and then fell at 24 h. p62 decreased at 6 h followed by restoration at 24 h (Fig. 1B, C). The results indicate that autophagic activity increased soon after PA stimulation began and then decreased with time. A potential association of USP10 and autophagic activity may exist. We investigated the role of autophagy in HepG2 cells treated with PA. The autophagy inhibitor bafilomycin A1 enhanced LD accumulation (Fig. 1D) and the autophagy agonist EBSS reduced LD accumulation (Fig. 1D). These results indicate that autophagy plays

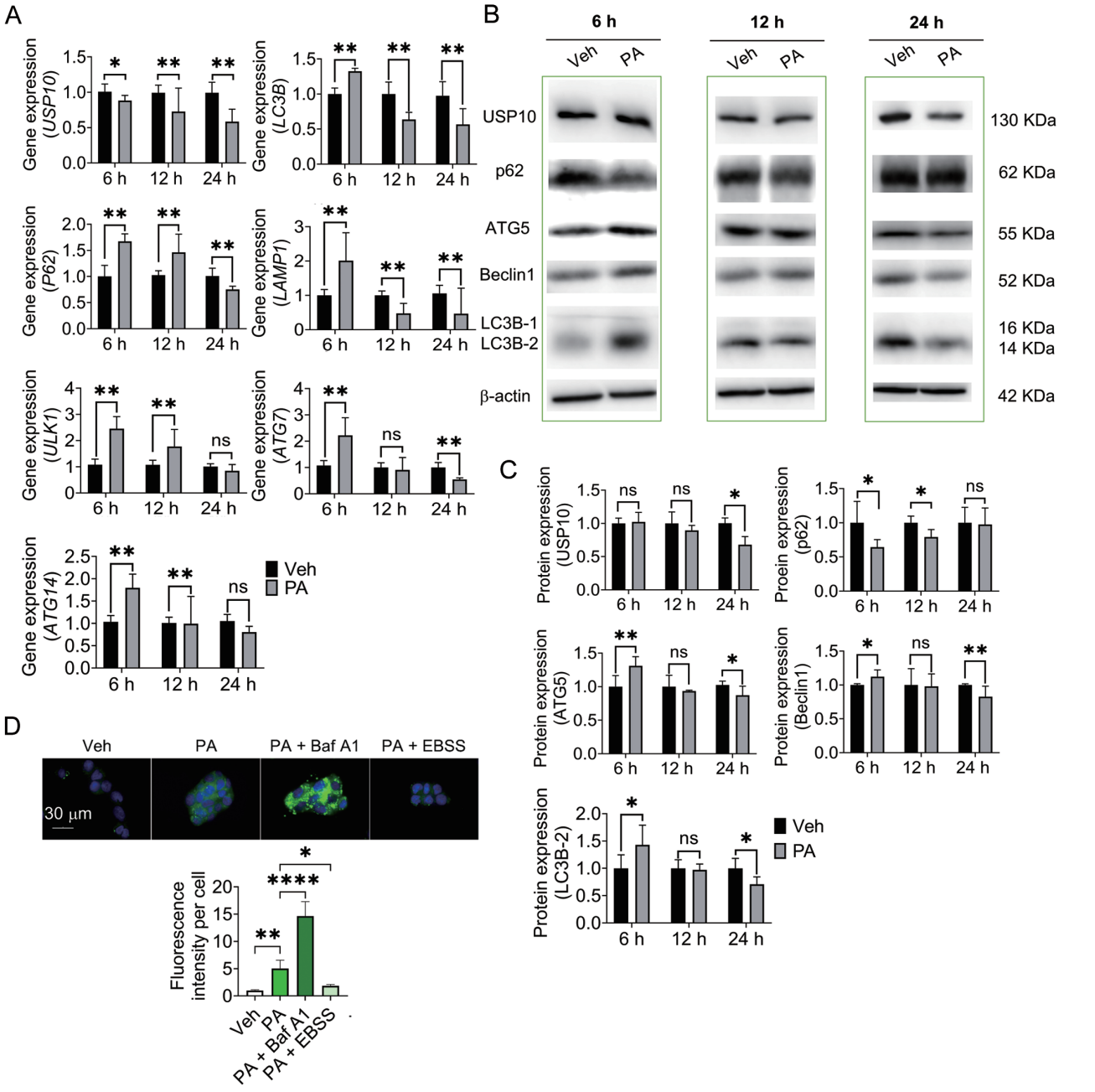

Fig. 1. PA affected autophagic activity and expression of USP10 of HepG2 cells. (A–C) HepG2 cells were treated with PA (312.5 μM) for 6, 12, or 24 h. Then, gene and protein expression were detected by quantitative polymerase chain reaction (qPCR) and western blotting. (A) Gene expression of *USP10, LC3B, p62, LAMP1, ULK1, ATG7* and *ATG14* in each group. Data are means±SD, n=3 (*p<0.05; **p<0.01; NS, not significant); (B, C) Protein expression of USP10, p62, ATG5, Beclin1 and LC3B-2 in each group. Data are mean±SD, n=3 (*p<0.05; **p<0.01; NS, not significant; (D) HepG2 cells were pretreated with EBSS for 2 h or bafilomycin A1 (Baf A1) (100 nM) for 5 h. HepG2 cells were treated with PA (312.5 μM) for an additional 24 h. LDs in HepG2 cells were stained by Bodipy 493/503. Nuclei were stained by DAPI. Bodipy 493/503 staining in each group are shown (*p<0.05; **p<0.01; ****p<0.0001; NS, not significant). ATG, autophagy target gene; EBSS, Earle's balanced salt solution; LAMP, lysosome-associated membrane protein; LC, microtubule-associated protein light chain; PA, palmitic acid; ULK, unc-51 like autophagy activating kinase; USP, ubiquitin-specific peptidase.

an essential role in hepatocellular steatosis.

PA inhibited autophagic flux of HepG2 cells

Autophagic flux reflects the dynamic process of autophagy process, which refers to synthesis of autophagosomes and their degradation. Blocking either one impairs autophagic flux, and fails to scavenge LDs in cells. Because CQ effectively increases lysosomal pH, and inhibits degradation of autophagosomes,[26] previous studies have it has been used to investigate autophagic flux in previous studies.[27,28] Supplementary Figure 2 shows how synthesis and degradation of autophagosomes can be detected with CQ.

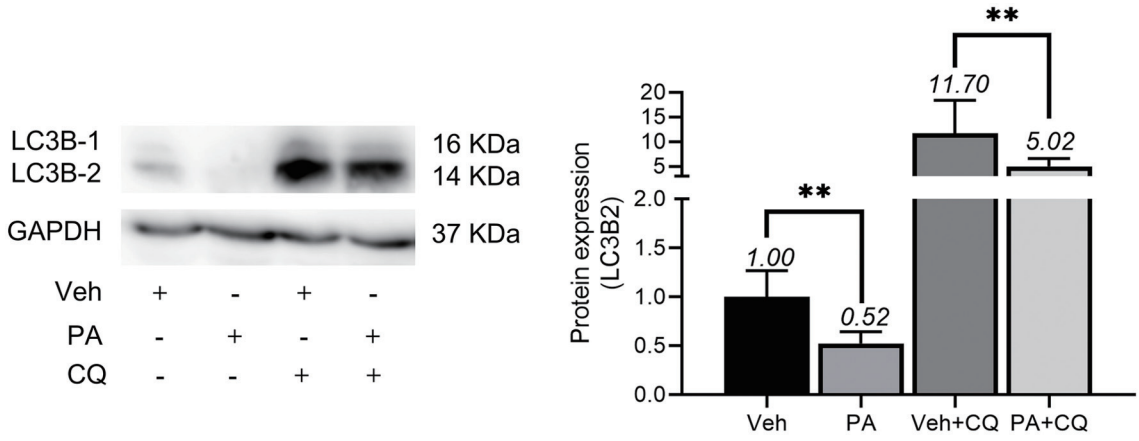

Fig. 2. Palmitic acid inhibited autophagic flux of HepG2 cells. HepG2 cells were pretreated with CQ (50 μM) for 6 h, followed by PA (312.5 μM) for an additional 24 h. LC3B-2 protein expression was assayed by western blotting. Italic numbers on histograms are average relative grayscale values. Data are means±SD, n=3 (**p<0.01). CQ, chloroquine diphosphate salt; LC, microtubule-associated protein light chain; PA, palmitic acid.

The effect of PA on autophagic flux in HepG2 cells was determined, and the average relative protein expression of LC3B-2 in each group is shown in Figure 2. In the presence of CQ, LC3B-2 expression was lower under PA stimulation compared with vehicle, suggesting that PA inhibited synthesis of autophagosomes. The decrease in LC3B-2 expression in the absence of CQ compared with the expression in the presence of CQ under PA stimulation was smaller compared with vehicle, suggesting that PA inhibited autophagosome degradation. Therefore, PA inhibited simultaneously inhibited the synthesis and degradation of autophagosomes.

USP10 restored autophagy in HepG2 cells

We established HepG2 cells with USP10 overexpression (USP10-OE) or USP10 knockdown (USP10-KD) through lentivirus infection. Two batches of HepG2 cells infected with USP10-sequence (LV-USP10) were established, Genechem-1 and Genechem-2. Western blotting showed that, compared with the control (LV-NC), USP10 level in Genechem-2 was higher than that in Genechem-1 (Supplementary Fig. 3A). Therefore, Genechem-2 was used in subsequent procedures in the USP10-OE model. HepG2 cells infected with three shRNAs targeting the USP10 gene (LV-shUSP10) were established, i.e. 4-1, 5-1, and 6-1. qPCR and western blotting showed that, compared with the control (LV-shScram), USP10 expression was the lowest in 5-1 (Supplementary Fig. 3B). Therefore, 5-1 was used subsequent procedures in the USP10-KD model.

Gain- and loss-of-function experiments were performed to ascertain whether USP10 regulated autophagic activity in HepG2 cells. qPCR showed that USP10-OE increased the expression of *LC3B*, *p62*, *LAMP1*, *ULK1,* and *ATG14*, but not *ATG7* compared with PA alone (Fig. 3A). Western blotting showed that USP10-OE increased the expression of LC3B-2, LAMP1, ATG5, and Beclin1, but not p62 compared with PA alone (Fig. 3B). qPCR showed that USP10-KD suppressed the expression of *LC3B*, *LAMP1*, *ATG7*, *ATG14,* and *p62*, but not *ULK1* compared with PA alone (Supplementary Fig. 4A). Western blotting showed that USP10-KD suppressed protein expression of LAMP1 and Beclin1, and promoted protein expression of p62 in contrast to PA-alone stimulation. Changes in LC3B-2 and ATG5 were not significant (Supplementary Fig. 4B). The results show that USP10 played a significant role in regulating autophagic activity of HepG2 cells under PA stimulation. 3-MA, an upstream inhibitor of autophagy,[26] was used to investigate whether USP10 regulated autophagic activity through the classic pathway. The increase in expression of VPS34, ATG5, Beclin1, and LC3B-2 induced by USP10 was inhibited by 3-MA (Fig. 4A). Also, as the efficacy and toxicity of 3-MA were debatable, shATG5 was used to block autophagosome formation. shATG5 significantly suppressed LC3B and USP10 was overexpressed (Fig. 4B). The results reveal that USP10 regulated autophagic activity through the classic autophagy pathway.

USP10 promoted autophagic flux in HepG2 cells

Western blotting and immunofluorescence were used to determine the effects of gain- and loss-of-function of USP10 on autophagic flux in HepG2 cells.

Western blotting: Supplementary Figure 2 illustrates how CQ was used to detect autosome synthesis and degradation. Average relative protein expression of LC3B-2 in each group is shown in Figure 5A and B. In the presence of CQ, the amount of LC3B-2 increased when USP10 was overexpressed compared with the expression in controls, whether or not the cells were treated with PA. The result suggests that USP10 promoted autophagosome synthesis. With PA treatment, difference in LC3B-2 expression in the absence of CQ compared with expression in the presence of CQ was greater in cells overexpressing USP10 compared with controls, suggesting that USP10 promoted of autophagosome degradation (Fig. 5A). In the presence of CQ, whether or PA was also present, LC3B-2 expression decreased when USP10 was knocked down compared with controls, suggesting that lack of USP10 inhibited autophagosome synthesis. In the presence of PA and USP10 knockdown, the difference in LC3B-2 expression in the absence of CQ was smaller than the expression when CQ was present, in contrast to controls. The result suggests that lack of USP10 inhibited autosomal degradation (Fig. 5B) and that USP10 simultaneously increased autophagosome synthesis and degradation.

Immunofluorescence: In the presence of CQ synthesized autophagosomes appear as red dots (LC3B) and lysosomes appear as green dots (LAMP1).[29] Autolysosomes appear as yellow dots, i.e. degraded autophagosomes. USP10-OE increased the numbers of red and yellow dots (Fig. 5C, D), and USP10 knockdown resulted in decreases in

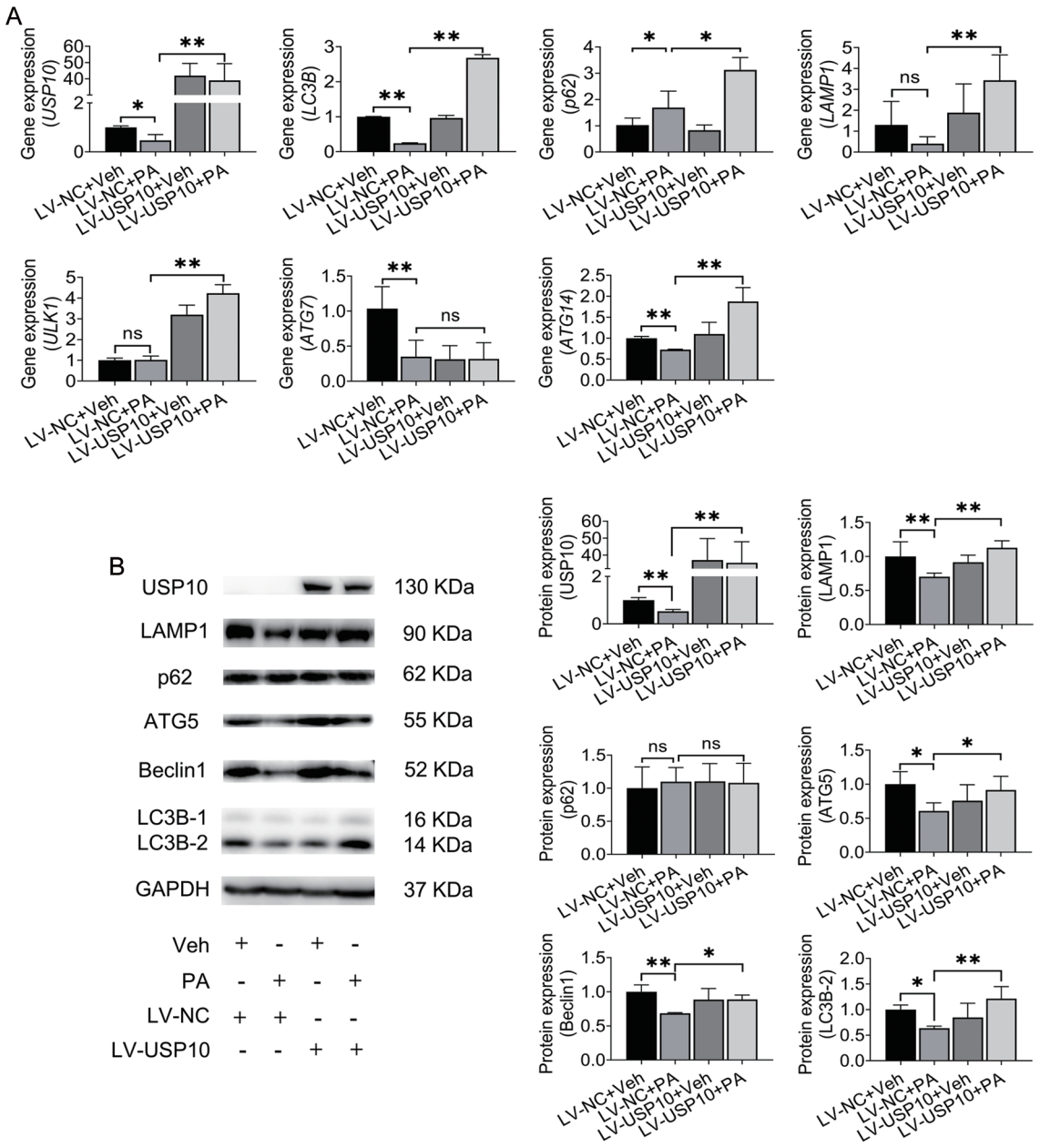

Fig. 3. USP10 restored autophagy in HepG2 cells. HepG2 cells overexpressing USP10- were treated with PA (312.5 μM) for 24 h. Gene and protein expression were assayed by qPCR and western blotting. (A, D) Gene expression of *USP10, LC3B, p62, LAMP1, ULK1, ATG7* and *ATG14* Data are means±SD, n=3 (*p<0.05; **p<0.01; NS, not significant). (B, C, E, F) Expression of USP10, LAMP1, p62, ATG5, Beclin1, and LC3B-2 expression. Data are mean±SD, n=4 (*p<0.05; **p<0.01; NS, not significant). ATG, autophagy target gene; LAMP, lysosome-associated membrane protein; LC, microtubule-associated protein light chain; PA, palmitic acid; ULK, unc-51 like autophagy activating kinase; USP, ubiquitin-specific peptidase.

the numbers of red and yellow dots decreased (Fig. 5C, D). USP10 thus increased autophagosome synthesis and degradation. Taken together, the results of western blotting and immunofluorescence confirmed the positive effect of USP10 on autophagic flux in HepG2 cells.

USP10 promoted LD-targeted autophagy of HepG2 cells

USP10-OE alleviated, and USP10-KD aggravated HepG2 cells steatosis (Fig. 6A), but the role of autophagy induced by USP10 in regulating intracellular LDs was not clear. The autophagy inhibitors bafilomycin A1, CQ, 3-MA, and shATG5 and agonists EBSS and rapamycin significantly reversed the effects of USP10-OE and USP10-KD on intracellular LDs (Fig. 6A, B). These results show that USP10 alleviated cellular steatosis that depended on autophagy. Specifically, USP10 regulated lipid-targeted autophagy. USP10-OE enhanced and USP10-KD abolished, colocalization of LC3B puncta and LAMP1 with LDs (Fig. 6C, D); USP10 thus promoted lipid-targeted autophagy in HepG2 cells.

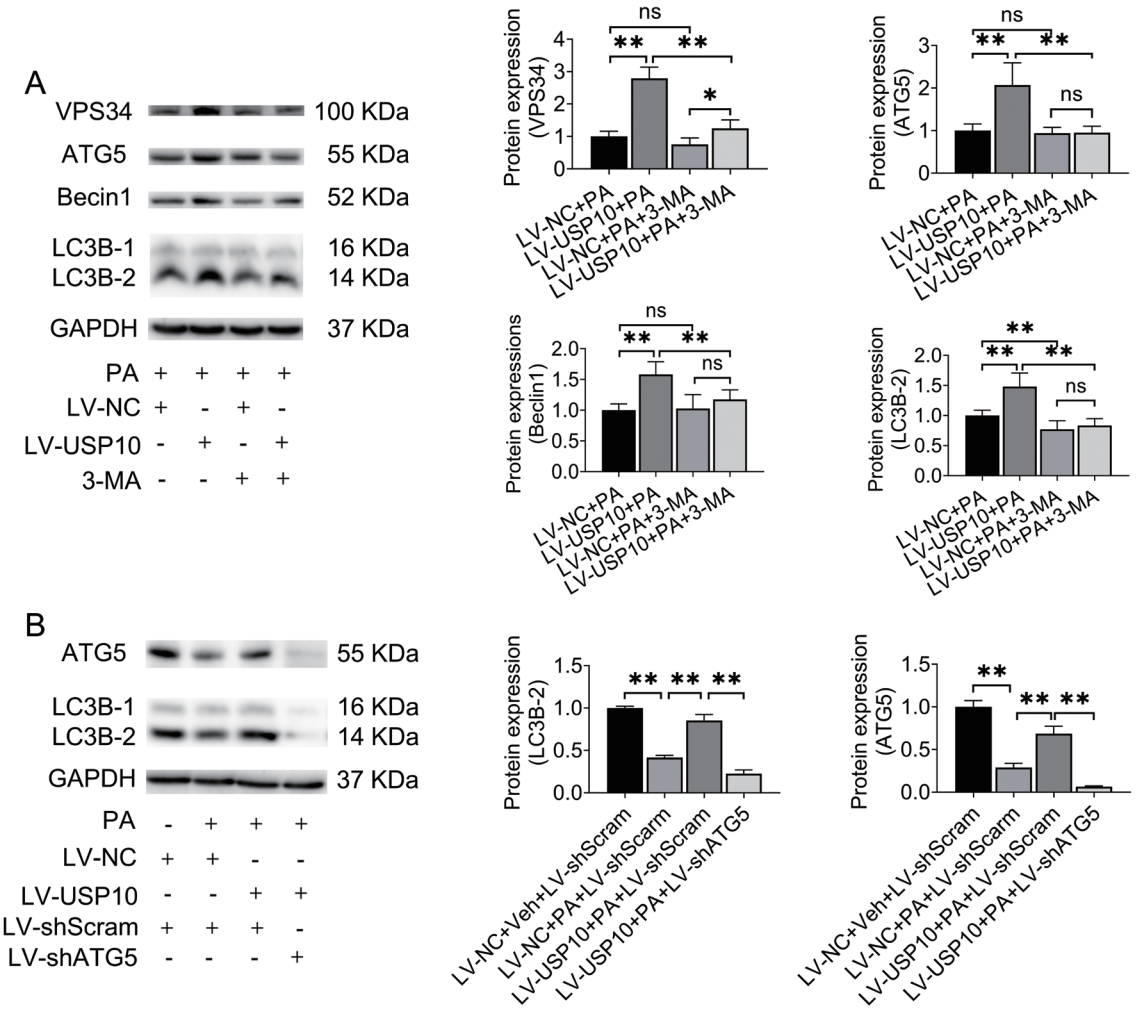

Fig. 4. USP10 restored autophagic activity of HepG2 cells through the classic autophagy pathway. HepG2 cells overexpressing USP10 were pretreated with 3-Methyladenine (3-MA) (5 mM) for 6 h, or shATG5 (MOI=20) for 12 h and treated with PA (312.5 μM) for an additional 24 h. Protein expression was assayed by western blotting. (A) Expression of VPS34, ATG5, Beclin1, and LC3B-2 protein. Data are means±SD, n=4 (*p<0.05; **p<0.01; NS, not significant). (B) Expression of ATG5 and LC3B-2 protein in. Data are means±SD, n=3 (**p<0.01). ATG, autophagy target gene; LC, microtubule-associated protein light chain; MOI, multiplicity of infection; PA, palmitic acid; USP, ubiquitin-specific peptidase; VPS34, phosphatidylinositol 3-kinase.

USP10 activated JNK1 and TSC2 signaling pathways to induce autophagy

We investigated whether USP10 regulated induction-stage autophagy. JNK1-Beclin1 and TSC2-mTOR are classic signaling pathways for inducing autophagy.[30] In contrast to treatment with PA alone, USP10-OE increased TSC2, JNK1, VPS34, and ATG14 protein expression accompanied by upregulation of the p-Bcl2/Bcl2 ratio and downregulation of the p-mTOR/mTOR and p-S6K/S6K ratios (Fig. 7A, B). The results show that USP10 activated the JNK1-Becin1 and TSC2-mTOR signaling pathways in HepG2 cells.

We also investigated whether USP10 induced autophagy that depended on JNK1. HepG2 cells were treated with DB07268, a specific inhibitor of JNK1[31] in the presence of PA. The concentration–viability curve is shown in Supplementary Figure 5, and the half maximal-inhibitory concentration (IC_{50}) of 90.51 μM. Subsequently, DB07268 at 1/10 (9 μM), 1/5 (18 μM), and 1/2 (45 μM) the IC50 was used to treat HepG2 cells. When USP10 was overexpressed, DB07268 significantly decreased JNK1 with dose-dependence (Fig. 8), but the changes in LC3B-2 and TSC2 were not consistent with those observed for JNK1. DB07268 (9–18 μM) did not significantly change TSC2 expression, but did increase LC3B-2. DB07268 (45 μM) inhibited both TSC2 and LC3B-2, and DB07268 (9–18 μM) treatment significantly increased the TSC2/JNK1 ratio (Fig. 8). We speculate that the rebound increase in LC3B-2 during DB07268 (9–18 μM) treatment was driven by compensatoryTSC2 expression against lack of JNK1. The compensatory expression of TSC2 was not observed when JNK1 was entirely inhibited entirely, leading to a rapid decrease in LC3B-2.

DB07268 treatment on HepG2 cells resulted in similar outcomes when USP10 was knocked down (Supplementary Fig. 6). The TSC2/JNK1 ratio was lower with DB07268 (9–18 μM) treatment than it was in cells overexpressing USP10 (Supplementary Fig. 6), which indicated that the degree of TSC2 compensatory expression was associated with the USP10 level. Immunofluorescence showed the strong colocalization of USP10 and TSC2 in HepG2 cells treated with DB07268 (18 μM) treatment (Supplementary Fig. 7). We thus speculate that the compensatory expression of TSC2 was directly mediated by USP10.

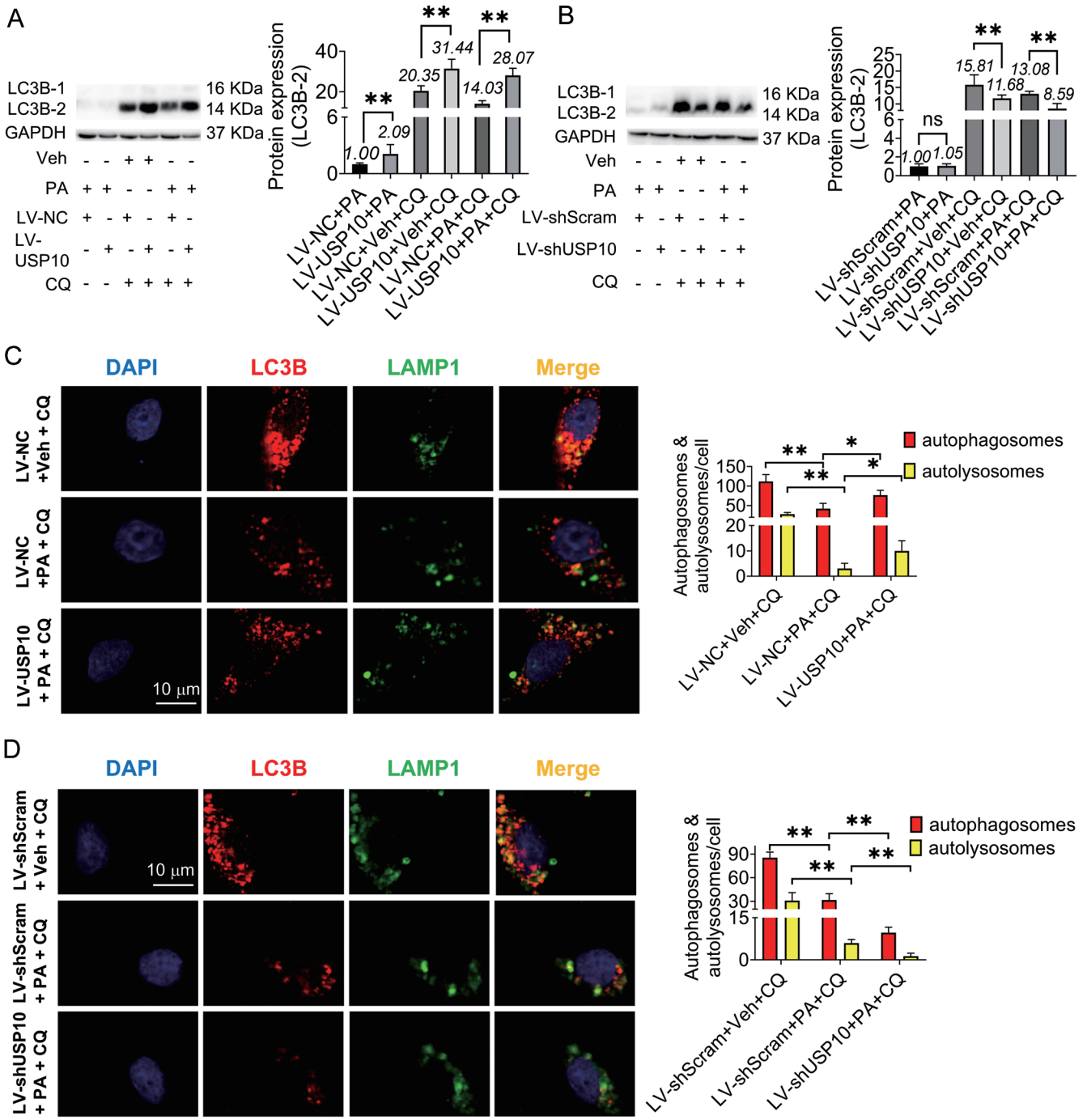

Fig. 5. USP10 promoted autophagic flux in HepG2 cells. HepG2 cells overexpressing USP10- or with USP10-knockdown were pretreated with CQ (50 μM) for 6 h, followed by PA (312.5 μM) for an additional 24 h. Protein expression was assayed by western blotting, with immunofluorescence staining of LC3B and LAMP1. (A, B) Expression of LC3B-2. Data are means±SD, n=6 (**p<0.01; NS, not significant). Italic numbers on histograms indicate average relative grayscale value in each group. (C, D) Immunofluorescence staining and counting of autophagosomes and autolysosomes. Nuclei were stained by DAPI. Data are means±SD, n=6 (*p<0.05; **p<0.01). CQ, chloroquine diphosphate salt; LAMP, lysosome-associated membrane protein; LC, microtubule-associated protein light chain; PA, palmitic acid; USP, ubiquitin-specific peptidase.

We determined whether the TSC2-to-JNK1 compensation was required for the rebound increase in LC3B-2. When TSC2 was knocked down, LC3B-2 decreased rapidly with DB07268 treatment without the rebound increase (Supplementary Fig. 8A). TSC2-to-JNK1 compensation was thus required to maintain LC3B-2 expression. Of note, in the absence of DB07268, expression of JNK1 and LC3B-2 induced by USP10 were not affected by TSC2 knockdown (Supplementary Fig. 8B). The results show that JNK1 was involved in the autophagy induced by USP10, and that TSC2 had an

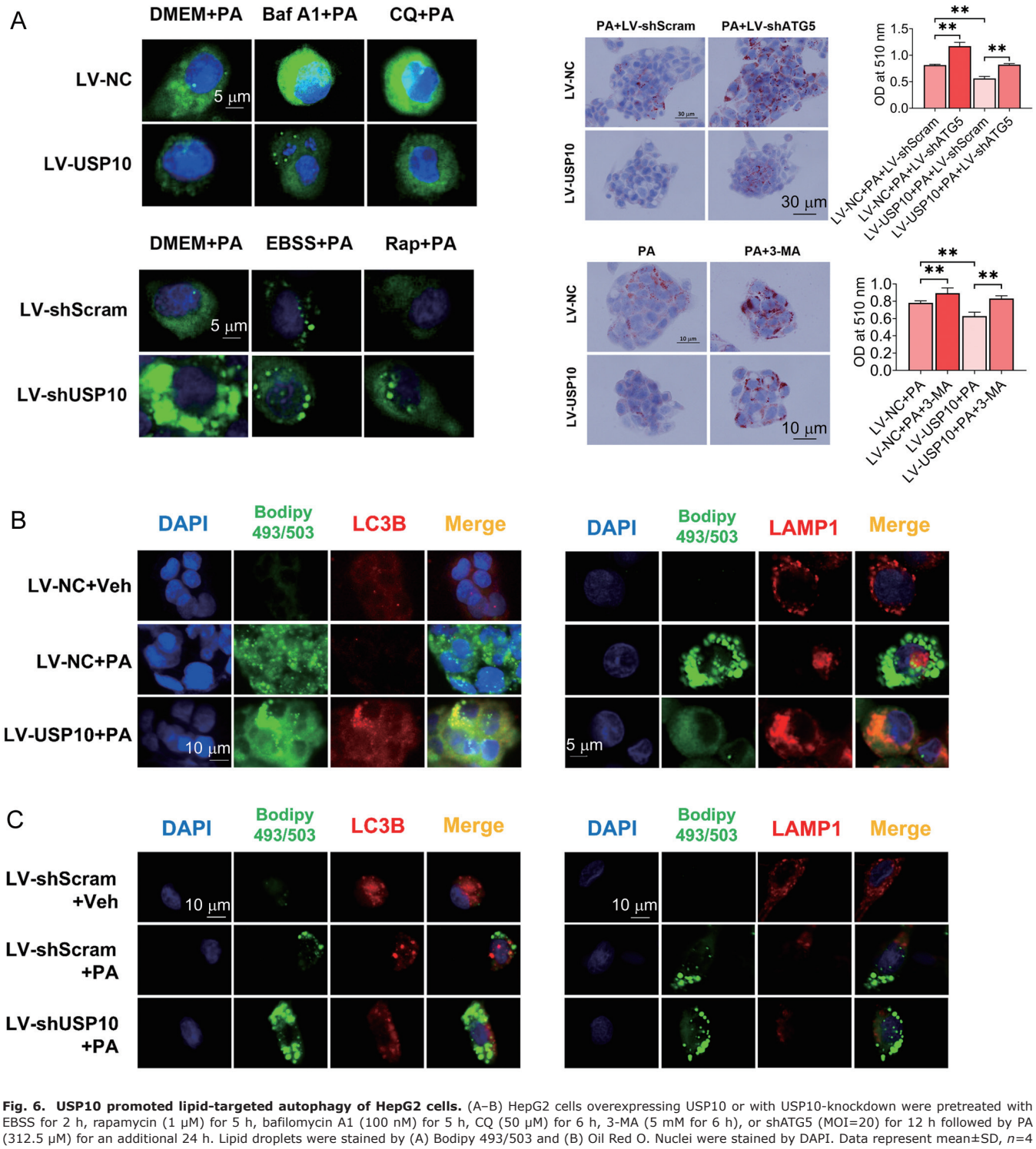

Fig. 6. USP10 promoted lipid-targeted autophagy of HepG2 cells. (A–B) HepG2 cells overexpressing USP10 or with USP10-knockdown were pretreated with EBSS for 2 h, rapamycin (1 μM) for 5 h, bafilomycin A1 (100 nM) for 5 h, CQ (50 μM) for 6 h, 3-MA (5 mM for 6 h), or shATG5 (MOI=20) for 12 h followed by PA (312.5 μM) for an additional 24 h. Lipid droplets were stained by (A) Bodipy 493/503 and (B) Oil Red O. Nuclei were stained by DAPI. Data represent mean±SD, n=4 (**p<0.01). (C–D) HepG2 cells overexpressing USP10 or with USP10-knockdown were treated with PA (312.5 μM) for 24 h. Lipid droplets, LC3B, and LAMP1 were stained fluorescently. (C, D) Fluorescence staining for Lipid droplets, LC3B and LAMP1. Nuclei were stained with DAPI. Baf A1, bafilomycin A1; CQ, chloroquine diphosphate salt; EBSS, Earle's balanced salt solution; LAMP, lysosome-associated membrane protein; LC, microtubule-associated protein light chain; MOI, multiplicity of infection; PA, palmitic acid; Rap, rapamycin; USP, ubiquitin-specific peptidase.

important supplementary role in maintaining autophagy. We also investigated whether the TSC2-to-JNK1 compensation impacted the lipid-lowering effect of USP10. When TSC2 was knocked down, DB07268 abolished the lipid-lowering effect of USP10 in a dose-dependent manner (Supplementary Fig. 9). The results show that the JNK1/TSC2 signaling pathway was required for USP10 to induce autophagy and scavenge LDs in HepG2 cells.

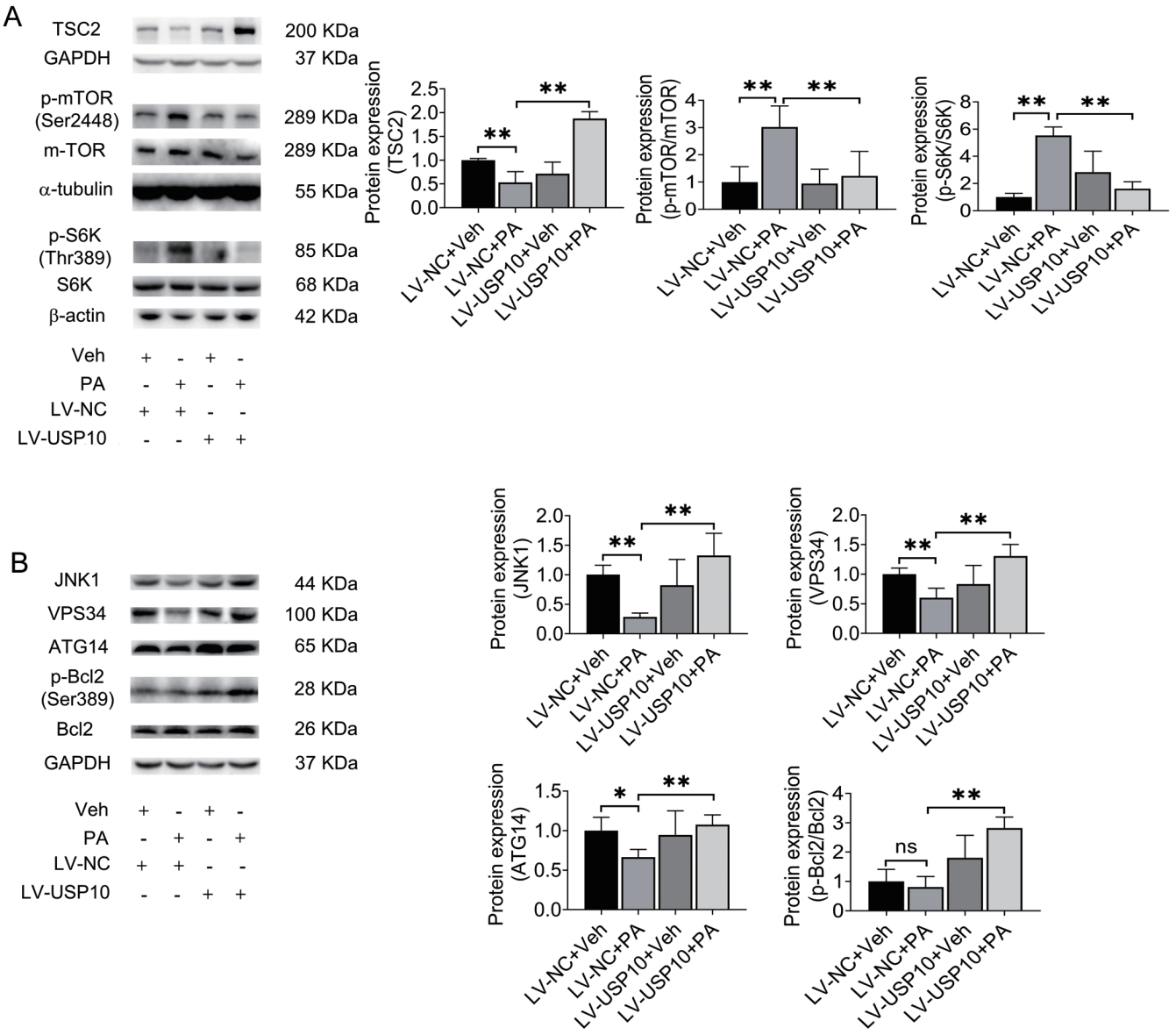

Fig. 7. USP10 activated TSC2 and JNK1 signaling pathways in HepG2 cells. HepG2 cells overexpressing USP10 were treated with PA (312.5 μM) for 24 h. Protein expression was assayed by western blotting. (A) Protein expression of tuberous sclerosis complex-2 (TSC2), mammalian target of rapamycin (mTOR), p-mTOR, ribosomal protein S6 kinase (S6K), and p-S6K. Data are means±SD, n=3 (**p<0.01). (B) Expression of C-jun N-terminal protein kinase-1 (JNK1), VPS34, ATG14, Bcl2, and p-Bcl2. Data are means±SD, n=3 (*p<0.05; **p<0.01; NS, not significant). ATG, autophagy target gene; JNK, C-jun N-terminal protein kinase; mTOR, mammalian target of rapamycin; S6K, ribosomal protein S6 kinase; TSC, tuberous sclerosis complex; USP, ubiquitin-specific peptidase; VPS34, phosphatidylinositol 3-kinase.

Discussion

NAFLD places an enormous burden on global healthcare. It can coexist with other metabolic syndromes including type 2 diabetes mellitus, obesity, and chronic cardiovascular disease, and contributes to a vicious cycle that increases liver-specific and overall mortality.[1] Although the two-hit theory is a cornerstone for pathogenesis of NAFLD, details need to be addressed. USP10 is a novel mediator of NAFLD that inhibits hepatic steatosis, insulin resistance, and inflammation. In this study, USP10 had positive effects on autophagy in HepG2 cells that were stimulated by PA, including restoration of autophagic activity, promoting autophagic flux, increasing lipid-targeted autophagy, and activating signaling pathways that promoted autophagy. Of note, we discovered TSC2-to-JNK1 compensation for maintaining autophagy that was associated with USP10 level. The collective effects on autophagy are important pathway of USP10 to alleviate steatosis in hepatocytes.

Autophagy has an essential role in NAFLD. Immunohistochemical staining of liver tissue from NASH patients has shown that the number of LC3B puncta was significantly decreased compared with normal controls.[32] In a mouse NASH model induced by a methionine- and choline-deficient diet, transmission electron microscopy showed a decrease in the number of autophagosomes and LC3B-2 expression in liver tissue.[33] In our study, HepG2 cells were used to model hepatocellular steatosis. PA suppresses autophagy, and leads to accumulation of LDs and lipotoxicity,[34] and in our study, PA

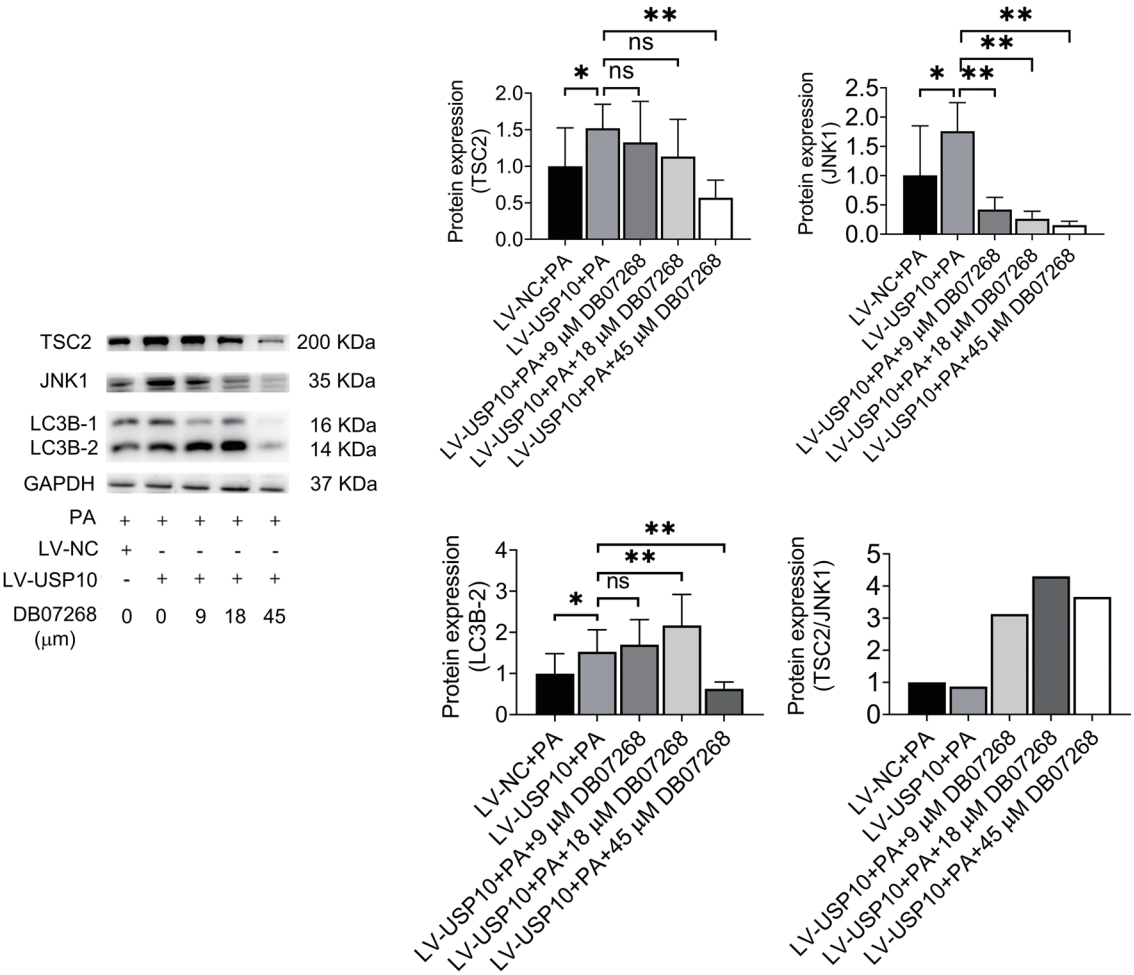

Fig. 8. USP10 mediated autophagy through JNK1. HepG2 cells overexpressing USP10- were treated with DB07268 (0–45 μM) for 24 h in the presence of PA (312.5 μM). Expression of TSC2, JNK1, and LC3B-2 protein was assayed by western blotting. Data are means±SD, n=4 (*p<0.05; **p<0.01; NS, not significant). LC, microtubule-associated protein light chain; JNK, C-jun N-terminal protein kinase; TSC, tuberous sclerosis complex; USP, ubiquitin-specific peptidase.

had time-dependent effects on autophagy in HepG2 cells. PA promoted autophagy at an early stage but autophagy was impaired later on. Similar results have been obtained in HL-7702, cells, L02 cells, and AML-12 cells.[8,35] Adenovirus-mCherry-GFP-LC3B has been used to measure autophagic flux,[36,37] but has some limitations. First, adenovirus-mCherry-GFP-LC3B cannot completely replace the endogenous LC3B in cells. Second, it is suitable for detecting autophagosome degradation but not synthesis. Co-immunofluorescence staining of LC3B puncta and LAMP1, and quantitative analysis of LC3B-2 protein expression,[38] are novel approaches to discriminate between disturbed autophagic initiation and lysosome function that were used in this study to evaluate autophagic flux. PA inhibited synthesis and degradation of autophagosomes. Specifically, colocalization of LC3B puncta and LAMP1 with LDs showed that PA inhibited lipid-targeted autophagy. The result is consistent with a previous study in which DAPGreen and LysoTracker were used to detect the effect of oleic acid on lipid-targeted autophagy.[10] Another study found that lipophagy was weakened in AML12 cells treated with oleic acid and PA, which supports our findings.[35]

USP10 plays is involved in tumorigenesis[39–41] and energy metabolism[16,20] in the liver. In this study, USP10 restored autophagy and promoted autophagic flux to alleviate hepatocellular steatosis. Of note, USP10 upregulated p62 gene expression, but did not affect its protein expression. We speculate that p62 was degraded during autophagic flux after its translation. In fact, autophagy cannot be evaluated based only on p62. p62 is a substrate protein and mediates binding of autophagosomes and their cargo.[4] Impaired autophagy induces p62 accumulation,[10,35] and a previous study found that p62 itself directly induced autophagy.[42] Therefore, it is hard to distinguish p62 protein as an outcome of impaired autophagy or as a requirement for autophagy activation.

USP10 regulates downstream molecules by post-translational modification, and a recent study reported that USP10 reduced the ubiquitination of LC3B-2 in H4 cells.[19] Other explanations of the how USP10 may have increased LC3B-2 include elevated LC3B gene expression in response to USP10 overexpression. A second explanation is that ATG5 and ATG7 gene and protein expression, which are involved in synthesis and maturity of LC3B-2 protein, were regulated by USP10. Third, USP10 promoted the expression of LC3B-2 protein, with dependence on VPS34 and ATG5. Signaling pathways associated with inducing autophagy were identified in our study. In the mTOR signaling pathway, USP10 decreased the p-mTOR/mTOR and p-S6K/S6K ratios in HepG2 cells. A previous study found that USP10 functioned as a tumor suppressor in hepatocellular carcinoma cells, stabilizing AMPKα by inhibiting its polyubiquitylation and negative

regulation of mTOR.[43] USP10 has been found to increase Beclin1, VPS34 and ATG14 simultaneously. USP10-OE was reported to reduce the levels of ubiquitinated Beclin1 in H4 and 293T cells, without affecting the ubiquitination of VPS34, ATG14 and p150, were not affected.[18] Post-translational modifications may thus be important, but not a unique mechanism, of the USP10 regulation of autophagy in HepG2 cells exposed to PA.

JNK1 and TSC2 are molecules upstream of Beclin1 and mTOR, and a JNK1 inhibitor was used to determine whether USP10 induced autophagy required JNK1. Previous studies have used SP600125 to inhibit JNK1-induced autophagy,[44,45] but SP600125 inhibits other JNK family members (JNK1, JNK2 and JNK3). DB07268 is a specific JNK1 inhibitor, and it revealed that USP10 induced autophagy that depended on JNK1 rather than TSC2. TSC2-to-JNK1 compensation was seen to maintain autophagy to some extent when JNK1 was inhibited. The extent of TSC2-to-JNK1 compensation was associated with the USP10 level. However, possible mechanisms of interaction among USP10, JNK1 and TSC2 have not been previously reported.

In our study, autophagic inhibitors and shATG5 decreased the protective effect of USP10 on LD accumulation. Lipid-targeted autophagy was promoted when USP10 was overexpressed, which makes autophagy a novel pathway for USP10 to alleviate hepatocellular steatosis. Lack of JNK1/TSC2 caused severe steatosis in HepG2 cells even if USP10 was overexpressed. As a consequence, USP10 had lipid-lowering effects in HepG2 cells through JNK1/TSC2-induced autophagy.

Conclusions

USP10 alleviated PA-induced hepatocellular steatosis through autophagy, USP10 restored autophagy, promoted autophagic flux, and increased lipid-targeted autophagy. JNK1/TSC2 signaling pathways were required for USP10 to achieve its lipid-lowering effect. Some limitations exist. First, experimental outcomes were only observed in HepG2 cells. Second, research on lipotoxicity, inflammation, and fibrosis induced by autophagy was lacking. Third, other special types of autophagy such as lipophagy and mitophagy were not investigated. The effect of USP10 on autophagy should be investigated in NAFLD rodent models and patients. Additional mechanisms of the regulation of JNK1, TSC2, and ATGs by USP10 should be investigated.

Acknowledgments

We thank Professor NP Wang and Professor L Jiao for their kind guidance in study design.

Funding

None to declare.

Conflict of interest

The authors have no conflicts of interest related to this publication.

Author contributions

Study concept and design (SLX), acquisition of data (SLX), analysis and interpretation of data (SLX), drafting of the manuscript (SLX, XLP), critical revision of the manuscript for important intellectual content (SLX, XLP, YYY), administrative, technical, or material support (YYY), and study supervision (YYY, XYX). All authors have made a significant contribution to this study and have approved the final manuscript.

Data sharing statement

The data used to support the findings of this study are available from the corresponding author upon request.

References

[1] Lombardi R, Iuculano F, Pallini G, Fargion S, Fracanzani AL. Nutrients, Genetic Factors, and Their Interaction in Non-Alcoholic Fatty Liver Disease and Cardiovascular Disease. Int J Mol Sci 2020;21(22):8761. doi:10.3390/ijms21228761, PMID:33228237.
[2] Pierantonelli I, Svegliati-Baroni G. Nonalcoholic Fatty Liver Disease: Basic Pathogenetic Mechanisms in the Progression From NAFLD to NASH. Transplantation 2019;103(1):e1–e13. doi:10.1097/TP.0000000000002480, PMID:30300287.
[3] Eslam M, Sanyal AJ, George J, International Consensus Panel. MAFLD: A Consensus-Driven Proposed Nomenclature for Metabolic Associated Fatty Liver Disease. Gastroenterology 2020;158(7):1999–2014.e1. doi:10.1053/j.gastro.2019.11.312, PMID:32044314.
[4] Ueno T, Komatsu M. Autophagy in the liver: functions in health and disease. Nat Rev Gastroenterol Hepatol 2017;14(3):170–184. doi:10.1038/nrgastro.2016.185, PMID:28053338.
[5] Mihaylova MM, Shaw RJ. The AMPK signalling pathway coordinates cell growth, autophagy and metabolism. Nat Cell Biol 2011;13(9):1016–1023. doi:10.1038/ncb2329, PMID:21892142.
[6] Singh R, Kaushik S, Wang Y, Xiang Y, Novak I, Komatsu M, *et al*. Autophagy regulates lipid metabolism. Nature 2009;458(7242):1131–1135. doi:10.1038/nature07976, PMID:19339967.
[7] Xiao Y, Liu H, Yu J, Zhao Z, Xiao F, Xia T, *et al*. MAPK1/3 regulate hepatic lipid metabolism via ATG7-dependent autophagy. Autophagy 2016;12(3):592–593. doi:10.1080/15548627.2015.1135282, PMID:26760678.
[8] Cheng C, Deng X, Xu K. Increased expression of sterol regulatory element binding protein-2 alleviates autophagic dysfunction in NAFLD. Int J Mol Med 2018;41(4):1877–1886. doi:10.3892/ijmm.2018.3389, PMID:29336468.
[9] Li D, Cui Y, Wang X, Liu F, Li X. Apple polyphenol extract alleviates lipid accumulation in free-fatty-acid-exposed HepG2 cells via activating autophagy mediated by SIRT1/AMPK signaling. Phytother Res 2021;35(3):1416–1431. doi:10.1002/ptr.6902, PMID:33037751.
[10] Chu Q, Zhang S, Chen M, Han W, Jia R, Chen W, *et al*. Cherry Anthocyanins Regulate NAFLD by Promoting Autophagy Pathway. Oxid Med Cell Longev 2019;2019:4825949. doi:10.1155/2019/4825949, PMID:30931080.
[11] Bhattacharya U, Neizer-Ashun F, Mukherjee P, Bhattacharya R. When the chains do not break: the role of USP10 in physiology and pathology. Cell Death Dis 2020;11(12):1033. doi:10.1038/s41419-020-03246-7, PMID:33277473.
[12] Takahashi M, Higuchi M, Makokha GN, Matsuki H, Yoshita M, Tanaka Y, *et al*. HTLV-1 Tax oncoprotein stimulates ROS production and apoptosis in T cells by interacting with USP10. Blood 2013;122(5):715–725. doi:10.1182/blood-2013-03-493718, PMID:23775713.
[13] Takahashi M, Higuchi M, Matsuki H, Yoshita M, Ohsawa T, Oie M, *et al*. Stress granules inhibit apoptosis by reducing reactive oxygen species production. Mol Cell Biol 2013;33(4):815–829. doi:10.1128/MCB.00763-12, PMID:23230274.
[14] Zhang DH, Zhang JL, Huang Z, Wu LM, Wang ZM, Li YP, *et al*. Deubiquitinase Ubiquitin-Specific Protease 10 Deficiency Regulates Sirt6 signaling and Exacerbates Cardiac Hypertrophy. J Am Heart Assoc 2020;9(22):e017751. doi:10.1161/JAHA.120.017751, PMID:33170082.
[15] Jiangqiao Z, Tianyu W, Zhongbao C, Long Z, Jilin Z, Xiaoxiong M, *et al*. Ubiquitin-Specific Peptidase 10 Protects Against Hepatic Ischaemic/Reperfusion Injury via TAK1 Signalling. Front Immunol 2020;11:506275. doi:10.3389/fimmu.2020.506275, PMID:33133065.
[16] Luo P, Qin C, Zhu L, Fang C, Zhang Y, Zhang H, *et al*. Ubiquitin-Specific Peptidase 10 (USP10) Inhibits Hepatic Steatosis, Insulin Resistance, and Inflammation Through Sirt6. Hepatology 2018;68(5):1786–1803. doi:10.1002/hep.30062, PMID:29698567.
[17] Zhang B, Li H, Li D, Sun H, Li M, Hu H. Long noncoding RNA Mirt2 upregulates USP10 expression to suppress hepatic steatosis by sponging miR-34a-5p. Gene 2019;700:139–148. doi:10.1016/j.gene.2019.02.096, PMID:30898698.
[18] Liu J, Xia H, Kim M, Xu L, Li Y, Zhang L, *et al*. Beclin1 controls the levels of p53 by regulating the deubiquitination activity of USP10 and USP13. Cell 2011;147(1):223–234. doi:10.1016/j.cell.2011.08.037, PMID:21962518.
[19] Jia R, Bonifacino JS. The ubiquitin isopeptidase USP10 deubiquitinates LC3B to increase LC3B levels and autophagic activity. J Biol Chem 2021;296:100405. doi:10.1016/j.jbc.2021.100405, PMID:33577797.

[20] Deng M, Yang X, Qin B, Liu T, Zhang H, Guo W, *et al*. Deubiquitination and Activation of AMPK by USP10. Mol Cell 2016;61(4):614–624. doi:10.1016/j.molcel.2016.01.010, PMID:26876938.
[21] Pingitore P, Sasidharan K, Ekstrand M, Prill S, Linden D, Romeo S. Human Multilineage 3D Spheroids as a Model of Liver Steatosis and Fibrosis. Int J Mol Sci 2019;20(7):1629. doi:10.3390/ijms20071629, PMID:30986904.
[22] Gomez-Lechon MJ, Donato MT, Martinez-Romero A, Jimenez N, Castell JV, O'Connor JE. A human hepatocellular in vitro model to investigate steatosis. Chem Biol Interact 2007;165(2):106–116. doi:10.1016/j.cbi.2006.11.004, PMID:17188672.
[23] Alnahdi A, John A, Raza H. Augmentation of Glucotoxicity, Oxidative Stress, Apoptosis and Mitochondrial Dysfunction in HepG2 Cells by Palmitic Acid. Nutrients 2019;11(9):1979. doi:10.3390/nu11091979, PMID:31443411.
[24] Zeng X, Zhu M, Liu X, Chen X, Yuan Y, Li L, *et al*. Oleic acid ameliorates palmitic acid induced hepatocellular lipotoxicity by inhibition of ER stress and pyroptosis. Nutr Metab (Lond) 2020;17:11. doi:10.1186/s12986-020-0434-8, PMID:32021639.
[25] Moravcova A, Cervinkova Z, Kucera O, Mezera V, Rychtrmoc D, Lotkova H. The effect of oleic and palmitic acid on induction of steatosis and cytotoxicity on rat hepatocytes in primary culture. Physiol Res 2015;64(Suppl 5):S627–636. doi:10.33549/physiolres.933224, PMID:26674288.
[26] Pasquier B. Autophagy inhibitors. Cell Mol Life Sci 2016;73(5):985–1001. doi:10.1007/s00018-015-2104-y, PMID:26658914.
[27] Rubinsztein DC, Cuervo AM, Ravikumar B, Sarkar S, Korolchuk V, Kaushik S, *et al*. In search of an "autophagomometer". Autophagy 2009;5(5):585–589. doi:10.4161/auto.5.5.8823, PMID:19411822.
[28] Song YM, Lee YH, Kim JW, Ham DS, Kang ES, Cha BS, *et al*. Metformin alleviates hepatosteatosis by restoring SIRT1-mediated autophagy induction via an AMP-activated protein kinase-independent pathway. Autophagy 2015;11(1):46–59. doi:10.4161/15548627.2014.984271, PMID:25484077.
[29] Cheng XT, Xie YX, Zhou B, Huang N, Farfel-Becker T, Sheng ZH. Revisiting LAMP1 as a marker for degradative autophagy-lysosomal organelles in the nervous system. Autophagy 2018;14(8):1472–1474. doi:10.1080/15548627.2018.1482147, PMID:29940787.
[30] Shi B, Ma M, Zheng Y, Pan Y, Lin X. mTOR and Beclin1: Two key autophagy-related molecules and their roles in myocardial ischemia/reperfusion injury. J Cell Physiol 2019;234(8):12562–12568. doi:10.1002/jcp.28125, PMID:30618070.
[31] Cui J, Yin S, Zhao C, Fan L, Hu H. Combining Patulin with Cadmium Induces Enhanced Hepatotoxicity and Nephrotoxicity In Vitro and In Vivo. Toxins (Basel) 2021;13(3):221. doi:10.3390/toxins13030221, PMID:33803748.
[32] Park HS, Song JW, Park JH, Lim BK, Moon OS, Son HY, *et al*. TXNIP/VDUP1 attenuates steatohepatitis via autophagy and fatty acid oxidation. Autophagy 2021;17(9):2549–2564. doi:10.1080/15548627.2020.1834711, PMID:33190588.
[33] Jin X, Gao J, Zheng R, Yu M, Ren Y, Yan T, *et al*. Antagonizing circRNA_002581-miR-122-CPEB1 axis alleviates NASH through restoring PTEN-AMPK-mTOR pathway regulated autophagy. Cell Death Dis 2020;11(2):123. doi:10.1038/s41419-020-2293-7, PMID:32054840.
[34] Nguyen TB, Olzmann JA. Lipid droplets and lipotoxicity during autophagy. Autophagy 2017;13(11):2002–2003. doi:10.1080/15548627.2017.1359451, PMID:28806138.
[35] Zhang T, Liu J, Shen S, Tong Q, Ma X, Lin L. SIRT3 promotes lipophagy and chaperon-mediated autophagy to protect hepatocytes against lipotoxicity. Cell Death Differ 2020;27(1):329–344. doi:10.1038/s41418-019-0356-z, PMID:31160717.
[36] Ikeda F. The anti-apoptotic ubiquitin conjugating enzyme BIRC6/BRUCE regulates autophagosome-lysosome fusion. Autophagy 2018;14(7):1283–1284. doi:10.1080/15548627.2018.1471311, PMID:29929453.
[37] Li R, Wang X, Wu S, Wu Y, Chen H, Xin J, *et al*. Irisin ameliorates angiotensin II-induced cardiomyocyte apoptosis through autophagy. J Cell Physiol 2019;234(10):17578–17588. doi:10.1002/jcp.28382, PMID:30793300.
[38] Mei S, Ni HM, Manley S, Bockus A, Kassel KM, Luyendyk JP, *et al*. Differential roles of unsaturated and saturated fatty acids on autophagy and apoptosis in hepatocytes. J Pharmacol Exp Ther 2011;339(2):487–498. doi:10.1124/jpet.111.184341, PMID:21856859.
[39] Zhu H, Yan F, Yuan T, Qian M, Zhou T, Dai X, *et al*. USP10 Promotes Proliferation of Hepatocellular Carcinoma by Deubiquitinating and Stabilizing YAP/TAZ. Cancer Res 2020;80(11):2204–2216. doi:10.1158/0008-5472.CAN-19-2388, PMID:32217697.
[40] Yang J, Meng C, Weisberg E, Case A, Lamberto I, Magin RS, *et al*. Inhibition of the deubiquitinase USP10 induces degradation of SYK. Br J Cancer 2020;122(8):1175–1184. doi:10.1038/s41416-020-0731-z, PMID:32015510.
[41] Yuan T, Chen Z, Yan F, Qian M, Luo H, Ye S, *et al*. Deubiquitinating enzyme USP10 promotes hepatocellular carcinoma metastasis through deubiquitinating and stabilizing Smad4 protein. Mol Oncol 2020;14(1):197–210. doi:10.1002/1878-0261.12596, PMID:31721429.
[42] Jeong SJ, Zhang X, Rodriguez-Velez A, Evans TD, Razani B. p62/SQSTM1 and Selective Autophagy in Cardiometabolic Diseases. Antioxid Redox Signal 2019;31(6):458–471. doi:10.1089/ars.2018.7649, PMID:30588824.
[43] Lu C, Ning Z, Wang A, Chen D, Liu X, Xia T, *et al*. USP10 suppresses tumor progression by inhibiting mTOR activation in hepatocellular carcinoma. Cancer Lett 2018;436:139–148. doi:10.1016/j.canlet.2018.07.032, PMID:30056112.
[44] Ke D, Ji L, Wang Y, Fu X, Chen J, Wang F, *et al*. JNK1 regulates RANKL-induced osteoclastogenesis via activation of a novel Bcl-2-Beclin1-autophagy pathway. FASEB J 2019;33(10):11082–11095. doi:10.1096/fj.201802597RR, PMID:31295022.
[45] Ke D, Zhu Y, Zheng W, Fu X, Chen J, Han J. Autophagy mediated by JNK1 resists apoptosis through TRAF3 degradation in osteoclastogenesis. Biochimie 2019;167:217–227. doi:10.1016/j.biochi.2019.10.008, PMID:31654668.